*Chapter – IV**

On Non-Newtonian Rabinowitsch Fluid Squeeze Film Lubrication Between Rough Circular Stepped Plates

---

*Part of this Chapter has been published in the journal **"Tribology Online"**, Vol.11 (4), 2016, pp. 519-526.

4.1 Introduction

Nowadays, the use of small amount of additives to the lubricants is becoming of growing interest. The flow behaviour of a Newtonian lubricant blended with various additives cannot be accurately described by the classical continuum theory. The viscosity of such lubricants exhibits a non-linear relationship between the shear stress and the shear strain rate. To study the performance of bearings lubricated with non-Newtonian lubricants, Rabinowitsch fluid model is one of the models is to establish non-linear relationship between the shear stress and the shear strain rate. The performance of slider bearing and journal bearing lubricated with non-Newtonian lubricants was studied by Hsu and Saibel (1965), Wada and Hayashi (1971) respectively. They found that the pressure distribution of pseudo plastic fluids decreases below that of Newtonian fluids whose viscosity is equal to the initial viscosity of pseudo plastic fluids and load carrying capacity and the frictional force also decreases. The following stress – strain relation holds for one dimensional fluid flow is as given in the equation (2.1.1) in which μ is the zero shear rate viscosity, κ the non-linear factor responsible for the non-Newtonian effects of the fluid which will be referred to as coefficient of pseudo plasticity in this chapter. This model can be applied to the Newtonian lubricant for $\kappa = 0$, dilatant lubricants for $\kappa < 0$ and pseudo plastic lubricants $\kappa > 0$. By applying this Rabinowitsch fluid model, many investigators have studied the effect of non-Newtonian lubricants on the performance characteristics of hydrodynamic thin film bearings, for example, the problems of slot entry in journal bearing by Sharma *et.al* (2000), the hydrostatic journal bearings by Sinhasan and Sha (1996), the journal bearings by Hsu.(1967) and Bourging and Gay (1994), the slider bearings by Hashimoto (1994), and Lin (2001), and circular-

disk squeeze film by Hashimoto (1994). Usha and Vimla (2000) studied the squeeze film lubrication between two plane annuli and between parallel plates by Hung (2009). In recent years, the study of the effect of surface roughness on hydrodynamic lubrication of various bearing system has been received much attention mainly because, in practice, most of the bearing surfaces are rough. There are number of earlier studies which describe the surface roughness effects. According to the recent experimental investigations (1988, 1995) base oil blended with long chained additives is found to improve the lubricating properties and to reduce friction and surface damage.

In this chapter, an attempt has been made to analyze the squeeze film characteristics between rough circular stepped plates lubricated with Rabinowitsch fluid model, which has not been studied so for.

4.2 Mathematical formulation of the problem.

Consider a squeeze film between two circular stepped plates approaching each other with a normal velocity $V\left(=-\frac{\partial h}{\partial t}\right)$. The surface of the lower circular plate (at z=0)is assumed to be rough as shown in Fig.4.1. The lubricant in the film region is considered to be non-Newtonian Rabinowitsch fluid. The basic equations governing the flow of an incompressible non-Newtonian Rabinowitsch fluid model under the usual assumptions of hydrodynamic lubrication applicable to thin film are given by

$$\frac{1}{r}\frac{\partial (ru)}{\partial r}+\frac{\partial w}{\partial z}=0, \qquad (4.2.1)$$

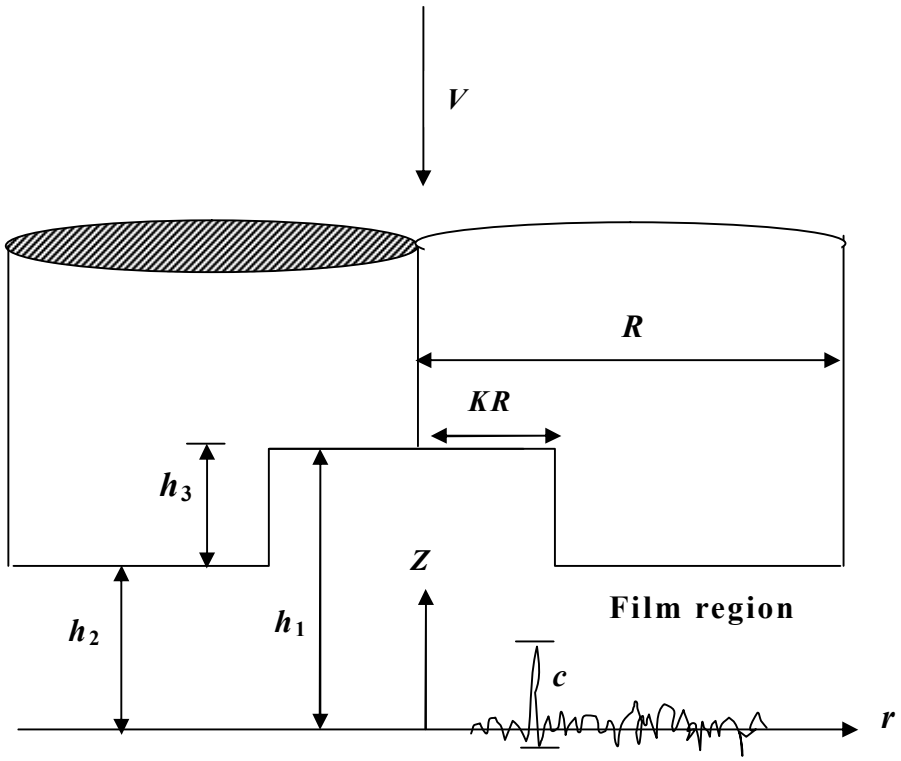

Figure 4.1 Squeeze film between rough circular stepped plates

$$\frac{\partial p}{\partial r} = \frac{\partial \tau_{xz}}{\partial z}, \tag{4.2.2}$$

$$\frac{\partial p}{\partial z} = 0. \tag{4.2.3}$$

The relevant boundary conditions for velocity components are

i. At the upper surface ($z = H$)

$$u = 0 \quad \text{and} \quad w = V = \left(-\frac{\partial H}{\partial t}\right), \tag{4.2.4a}$$

ii. At the lower surface ($z = 0$)

$$u = 0 \quad \text{and} \quad w = 0. \tag{4.2.4b}$$

To mathematically model the surface roughness the film thickness H is to be made up of two parts

$$H_i = h_i + h_s(r,\theta,\xi) \quad i = 1,2 \tag{4.2.5}$$

Where h_i denotes the nominal smooth part of the film geometry while h_s is the part due to the surface roughness and is measured from the nominal level. Without loss of generality it may be assumed that the mean value of h_s over bearing surface is zero.

4.3 Solution of the problem

Integrating equation (4.2.2) with respect to z subject to the boundary conditions (4.2.4a) and (4.2.4b) and using the constitutive equation (2.1.1), the expression for velocity component can be obtained as

$$u = \frac{1}{\mu}\left[\frac{1}{2}\left(\frac{\partial p}{\partial r}\right) z(z-H) + \kappa\left(\frac{\partial p}{\partial x}\right)^2 \left\{\frac{z^2}{4} - \frac{1}{2}z^2 H + \frac{3}{8}z^2 H^2 - \frac{1}{8}zH^2\right\}\right]. \tag{4.3.1}$$

Using equation (4.3.1) in the continuity equation (4.2.1) and integrating with respect to *z* under the relevant boundary conditions (4.2.4a) and (4.2.4b) for *z,* the modified Reynolds equation for non-Newtonian Rabinowitsch fluid is obtained in the form

$$\frac{1}{r}\frac{\partial}{\partial r}\left[r\left\{ H^3\left(\frac{\partial p}{\partial r}\right)+\frac{3}{20}\kappa H^5\left(\frac{\partial p}{\partial r}\right)^3\right\}\right]=-12\mu\frac{\partial H}{\partial t} \qquad (4.3.2)$$

4.4 Stochastic Reynolds equation

Let $f(h_s)$ be the probability density function of the stochastic film thickness h_s, taking the stochastic average of (4.3.2) with respect to $f(h_s)$, the averaged modified Reynolds type equation is obtained in the form

$$\frac{1}{r}\frac{\partial}{\partial r}\left[r\left\{ E(H^3)\left(\frac{\partial E(p)}{\partial r}\right)+\frac{3}{20}\kappa E(H^5)\left(\frac{\partial E(p)}{\partial r}\right)^3\right\}\right]=-12\mu\frac{\partial H}{\partial t} \qquad (4.4.1)$$

where the expectancy operator $E(\bullet)$ is defined by

$$E(\bullet)=\int_{-\infty}^{\infty}(\bullet)f(h_s)dh_s \qquad (4.4.2)$$

In accordance with the Christensen (1969-70), it is assumed that

$$f(h_s)=\begin{cases}\dfrac{35}{32c^7}(c^2-h_s^2)^3. & -c<h_s<c\\ 0 & \text{elsewhere}\end{cases} \qquad (4.4.3)$$

where $\sigma=c/3$ is the standard deviation.

In the context of Christensen (1969-70) stochastic theory for the hydrodynamic lubrication of rough surfaces, two types of one- dimensional surface roughness patterns are considered. Viz. radial roughness pattern and azimuthal roughness pattern.

Radial roughness pattern

For one dimensional radial roughness pattern, the roughness structure has the form of long narrow ridges and valleys running in the radial direction (i.e. they are straight ridges and valleys passing through $z = 0$, $r = 0$ to form star pattern), in this case the film thickness takes the form

$$H_i = h_i + h_s(\theta, \xi) \qquad i = 1,2$$

and stochastic modified Reynolds equation takes the form

$$\frac{1}{r}\frac{\partial}{\partial r}\left[r\left\{ E(H^3)\left(\frac{\partial E(p)}{\partial r}\right) + \frac{3}{20}\kappa\, E(H^5)\left(\frac{\partial E(p)}{\partial r}\right)^3 \right\}\right] = -12\mu V \qquad (4.4.4)$$

Azimuthal roughness pattern

For one dimensional azimuthal roughness, the bearing surface is assumed to have the form of long narrow ridges and valleys running in the θ - direction (*i.e* they are circular ridges and valleys on the circular plate that are concentric on $z = 0$, $r = 0$) In this case, film thickness is described by the function of the form

$$H_i = h_i + h_s(r, \xi) \qquad i = 1,2$$

and stochastic modified Reynolds equation takes the form

$$\frac{1}{r}\frac{\partial}{\partial r}\left[r\left\{ \frac{1}{E\left(\frac{1}{H^3}\right)}\left(\frac{\partial E(p)}{\partial r}\right)+\frac{3}{20}\kappa\frac{1}{E\left(\frac{1}{H^5}\right)}\left(\frac{\partial E(p)}{\partial r}\right)^3 \right\}\right]=-12\mu V. \qquad (4.4.5)$$

For an axisymmetric case, equations (4.4.4) and (4.4.5) together can be written as

$$\frac{1}{r}\frac{\partial}{\partial r}\left[r\left\{ \left(G\left(H,c\right)\right)^3\left(\frac{\partial E(p)}{\partial r}\right)+\frac{3}{20}\kappa\left(G\left(H,c\right)\right)^5\left(\frac{\partial E(p)}{\partial r}\right)^3 \right\}\right]=-12\mu V \qquad (4.4.6)$$

where

$$G(H,c)=\begin{cases} E(H). & \text{for radial roughness} \\ \left[E\left(\frac{1}{H}\right)\right]^{-1} & \text{for azimuthal roughness} \end{cases}$$

$$E(H)=\frac{35}{32c^7}\int_{-c}^{c} H(c^2-h_s^2)^3\,dh_s, \qquad (4.4.7)$$

$$E\left(\frac{1}{H}\right)=\frac{35}{32c^7}\int_{-c}^{c}\frac{(c^2-h_s^2)^3}{H}\,dh_s, \qquad (4.4.8)$$

Equation (4.4.6) is a non-linear equation in p, so the small perturbation method is used to find its solution.

The squeeze film pressure can be perturbed as

$$p=p_{00}+\kappa p_{01} \qquad (4.4.9)$$

Using equation (4.4.9) in the Reynolds type equation (4.4.6) and neglecting higher order terms of κ, two governing equations for squeeze film pressure p_{00} and p_{01} can be obtained respectively as

$$\frac{1}{r}\frac{d}{dr}\left[r\left(G(H,c)\right)^3\left(\frac{dp_{00}}{dr}\right)\right]=-12\mu\frac{\partial H}{\partial t} \tag{4.4.10}$$

$$\frac{1}{r}\frac{d}{dr}\left[\frac{3}{20}\left(G(H,c)\right)^5\left(\frac{dp_{00}}{dr}\right)^3+\left(G(H,c)\right)^3\left(\frac{dp_{01}}{dr}\right)\right]=0 \tag{4.4.11}$$

By using boundary condition

$$\frac{dE(p)}{dr}=0 \text{ at } r=0, \tag{4.4.12}$$

the modified Reynolds type equation for squeeze film pressure is obtained from the equations (4.4.10) and (4.4.11) in the form

$$\frac{dE(p_{00i})}{dr}=\frac{-6\mu Vr}{\left(G_i\left(H_i,c\right)\right)^3} \quad , \tag{4.4.13}$$

$$\frac{dE(p_{01i})}{dr}=\frac{162}{5}\frac{\mu Vr^3}{\left(G_i\left(H_i,c\right)\right)^7} \quad , \tag{4.4.14}$$

where

$h_1=h_2$ and $p_{ji}=p_{001}=p_{011}$ for the region $0\le r\le KR$

$h_1=h_2$ and $p_{ji}=p_{002}=p_{012}$ for the region $KR\le r\le R$

.

$$G_i\left(H_i\,c\right)=\begin{cases}E(H_i). & \text{for radial roughness}\\ \left[E\left(\frac{1}{H_i}\right)\right]^{-1} & \text{for azimuthal roughness}\end{cases}$$

With $H_i=h_i+h_s$, p_{0j1} and p_{0j2} (for j = 00,01) being the pressure in the region-I ($0\le r\le KR$) and in the region-II ($KR\le r\le R$) respectively.

The relevant boundary conditions for pressure are

$$E\left(p_{0j1}\right)=E\left(p_{0j2}\right) \quad \text{at} \quad r=KR, \tag{4.4.15a}$$

$$E\left(p_{0j2}\right)=0 \quad \text{at} \quad r=R. \tag{4.4.15b}$$

The solutions of equations (4.4.13) and (4.4.14) subject to the boundary conditions given in equations (4.4.15a) and (4.4.15b) is

For the Region- I, the fluid film pressure $E(p)=E(p_1)$ is obtained as

$$\left.\begin{aligned} E(p_1)=3\mu V&\left[\frac{K^2R^2-r^2}{\left(G_1(H_1,c)\right)^3}+\frac{R^2(1-\mathrm{K}^2)}{\left(G_2(H_2,c)\right)^3}\right] \\ -\frac{81}{10}\kappa\ \mu V&\left[\frac{K^4R^4-r^4}{\left(G_1(H_1,\,c)\right)^7}+\frac{R^4(1-\mathrm{K}^4)}{\left(G_2(H_2,c)\right)^7}\right] \end{aligned}\right\} \tag{4.4.16}$$

and for the Region- II $E(p)=E(p_2)$ is obtained as

$$E(p_2)=3\mu V\left[\frac{R^2-r^2}{\left(G_2(H_2\ c)\right)^3}\right]-\frac{81}{10}\kappa\ \mu V\left[\frac{R^4-r^4)}{\left(G_2(H_2\ c)\right)^7}\right] \tag{4.4.17}$$

The non-dimensional pressure in the region- I given in equation (4.4.16) and in the region -II given in equation (4.4.17) are obtained in the form

$$E(p_1^*)=\frac{2E(p_1)}{3\mu VR^2}=\left\{\frac{(K^2-r^{*2})}{h_1^3}+\frac{(1-K^2)}{h_2^3}\right\}-\frac{81\alpha}{5}\left\{\frac{(K^4-r^{*4})}{h_1^7}+\frac{(1-K^4)}{h_2^7}\right\},$$

$$E(p_2^*)=\frac{2E(p_2)}{3\mu VR^2}=\left\{\frac{(1-r^{*2})}{h_2^3}\right\}-\frac{81\alpha}{5}\left\{\frac{(1-r^{*4})}{h_2^7}\right\},$$

where

$$\alpha=\kappa^*R^2,\quad r^*=\frac{r}{R}\quad h_1^*=\frac{h_1}{h_0},\quad h_2^*=\frac{h_2}{h_0}.$$

The load carrying capacity $E(W)$ is obtained by

$$E(W) = 2\pi \int_0^{KR} rE(p_1)dr + 2\pi \int_{KR}^{R} rE(p_2)dr. \qquad (4.4.18)$$

The non-dimensional load carrying capacity W^* is obtained in the form

$$W^* = \frac{E(W)h_2^3}{3\pi\mu VR^4} = \left\{\frac{K^4}{G_1(H^*\ c)} + \frac{(1-\mathrm{K}^4)}{G_2(1\ c)}\right\} - \frac{81}{5}\alpha\left\{\frac{K^6}{G_1(H^*\ c)} + \frac{(1-\mathrm{K}^6)}{G_2(1\ c)}\right\} \qquad (4.4.19)$$

Writing $V = -\frac{dh}{dt}$ in the equation (4.4.19) the squeeze film time for reducing the film thickness from the initial value h_0 of h_2 to a final value h_f is given by

$$t = \frac{-3\mu\pi R^4}{2E(W)} = \int_{h_0}^{h_f} \left[\begin{array}{l} \left\{\frac{K^4}{\left(G_1(H_1,c)\right)^3} + \frac{1-K^4}{\left(G_2(H_2,c)\right)^3}\right\} \\ -\frac{81}{5}\kappa\ R^2\left\{\frac{K^6}{\left(G_1(H_1,c)\right)^7} + \frac{1-K^6}{\left(G_2(H_2,c)\right)^7}\right\} \end{array}\right] dh_2 \qquad (4.4.20)$$

which in the non- dimensional form is obtained as

$$t^* = \frac{2E(W)h_0^2 t}{3\mu\pi R^3} = \int_{h_f^*}^{1} \left[\begin{array}{l} \left\{\frac{K^4}{\left(G_1(h_2^*,h_3^*h_s^*,C)\right)^3} + \frac{1-K^4}{\left(G_2(h_2^*,h_s^*,C)\right)^3}\right\} \\ -\frac{18}{5}\alpha\left\{\frac{K^6}{\left(G_1(h_2^*,h_3^*h_s^*,C)\right)^7} + \frac{1-K^6}{\left(G_2(h_2^*,h_s^*,C)\right)^7}\right\} \end{array}\right] dh_2^*, \qquad (4.4.21)$$

where $h_f^* = \frac{h_f}{h_0}$; $h_2^* = \frac{h_2}{h_0}$; $h_s^* = \frac{h_s}{h_0}$ $C = \frac{c}{h_0}$ $h_3^* = \frac{h_3}{h_0}$.

In the limiting case of the roughness parameter $C \to 0$, the expressions for pressure, load carrying capacity and squeeze film time reduce to those obtained for the smooth case, studied by Naduvinamani *et. al*. (2014).

4.5 Results and discussions

In the present analysis, the effect of surface roughness on the squeeze film characteristics between circular stepped plates lubricated with Rabinowitsch fluid model is presented on the basis of the Christensen stochastic theory for the study of rough surfaces. This section is devoted to the discussion of graphical results for non dimensional load carrying capacity and squeeze film time. The effects of surface roughness parameter C and the non linear factor α are analyzed. It is observed that all the squeeze film characteristics are found to be functions of non-linear factor α of the lubricant and the roughness parameter C. As the value α approaches to zero, the non-dimensional Reynolds equation reduces to that of the Newtonian lubricant case and the limiting case of $C \to 0$ corresponds to smooth case studied by Naduvinamani *et. al*.(2014)

In order to analyze the non-Newtonian effects of the fluids on the squeeze film performance of circular stepped plates, various squeeze film characteristics are presented with the following numerical values.

i. Dimensionless non-linear factor α = - 0.01 to 0.01.

ii. Step- height K = 0.2 to 0.6.

iii. Dimensionless roughness parameter C = 0.2 to 0.4.

4.5.1 Load carrying capacity

The variation of non-dimensional load carrying capacity W^* with H^* for different values of α with K= 0.5 and C = 0.1 is shown in Fig. 4.2 for both the radial and azimuthal roughness patterns. It is clear from the figure that, the load carrying capacity W^* decreases for increasing value of H^* for both radial and azimuthal roughness patterns. Further, it is also observed that in case of shear thickening fluid (dilatant) the flow motion of lubricants is relatively slow as compared to shear thinning fluids, which contributes in the increase of squeeze film pressure for dilatant fluids and a decrease in squeeze film pressure for shear thinning fluids and hence the non-dimensional load carrying capacity W^* increases for dilatant fluids $(\alpha < 0)$ and decreases for pseudo plastic fluids $(\alpha > 0)$ for both the type of roughness patterns. Increasing the roughness asperities heights running in the form of long narrow ridges and valleys running in the radial direction (radial roughness) forming a star pattern and causes the easy passage for the lubricant to escape in the radial direction and hence decreases the squeeze film pressure, by which decreases the load carrying capacity. Hence the increase in load carrying capacity is more accentuated for the azimuthal roughness pattern than the radial roughness pattern.

The variation of non-dimensional load carrying capacity W^* with H^* for different values of K with $\alpha = 0.01$ and C = 0.2 is shown in Fig. 4.3 for both type of roughness patterns. It is observed that, W^* decreases for increasing values of K. The increasing value of K leads to increase in the step region and hence increases the area of the fluid film region and thus decreases the pressure and by which decreases the load carrying capacity.

Figure 4.4 depicts the variation of W^* with H^* for different values of the roughness parameter *C*. Increasing the roughness asperities heights running in the form of long narrow ridges and valleys running in the azimuthal direction (azimuthal roughness) causes the more resistance for the lubricant to squeeze out from the film region and hence increases the squeeze film pressure, by which increases the load carrying capacity. However increasing the roughness asperities heights running in the form of long narrow ridges and valleys running in the radial direction (radial roughness) forming a star pattern and causes an easy passage for the lubricant to escape in the radial direction and hence decreases the squeeze film pressure, by which decreases the load carrying capacity W^*. It is observed that, increasing values of roughness parameter *C*, the load carrying capacity W^* increases (decreases) for azimuthal (radial) roughness pattern.

4.5.2 Squeeze film time

Figure 4.5 shows the variation of non dimensional squeeze film time t^* with h_f^* for different values of non linear factor $t^*$with fixed values of roughness parameter $C = 0.2$, $K = 0.5$ and $h_3^* = 0.15$. In both type of roughness patterns it is observed that, significant increase in response time $t^*$for dilatant fluids as compared to the Newtonian case this is because in the case of shear thickening fluids more resistance is observed for the movement of plates and increases the load carrying capacity and hence delayed time of approach is observed. However, in the case of shear thinning fluids load carrying capacity decreases and hence squeezing time decreases as compared to the corresponding Newtonian case. Also one can observe that, the increase (decrease) in t^* is more for azimuthal (radial) roughness patterns.

Figure 4.6 depicts the variation of non- dimensional squeeze film time t^* with h_f^* for different values of K with $\alpha = 0.01$, $C = 0.2$ and $h_3^* = 0.15$ as the values of K increases the squeeze film time decreases in both radial and azimuthal roughness patterns. The variation of non – dimensional squeeze film time t^* with h_f^* for different values of roughness parameter C with fixed values of $\alpha = 0.01$, $K = 0.4$ and $h_3^* = 0.15$ is shown in Fig.4.7 and Fig.4.8 respectively for the shear thinning and shear thickening lubricants. It is observed that, as the roughness parameter C increases the squeeze film time t^* increases (decreases) for radial (azimuthal) roughness pattern in case of shear thinning fluids (pseudo plastic fluids, $(\alpha > 0)$, where as the reverse trend is observed for the shear thickening fluids (dilatant lubricants, $(\alpha < 0)$.

4.6 Conclusions

The influence of surface roughness on squeeze film characteristics between circular stepped plates with Rabinowitsch fluid model is presented. The averaged modified Reynolds equations for both types of roughness patterns are derived. The non-linear Reynolds type equations are solved by using the small perturbation technique. The results are in well agreement with the Newtonian case and also with the smooth case studied by Naduvinamani *et. al*. (2014). Based on the numerical results, presented in the above section, following conclusions have been drawn.

i. The increased load carrying capacity is observed for shear thickening (dilatant) lubricants whereas the reverse trend is observed for the shear thinning fluids (pseudoplastic lubricants).

ii. There is a significant increase in the squeeze film time for dilatant lubricants as compared with the Newtonian case, squeeze film time decreases for the pseudo plastic lubricants.

iii. The effect of azimuthal (radial) roughness pattern is to increase (decrease) the load carrying capacity and squeeze film time as compared to the smooth case.

iv. As the squeezing time of the rough circular stepped plates system is significantly increases with the dilatants lubricants and hence it is expected that the use of additives can reduce the vibrations in the respective systems.

Hence, the results so obtained are more helpful for better bearing performance and stability. So the present results are expected to be closer to the physical situation.

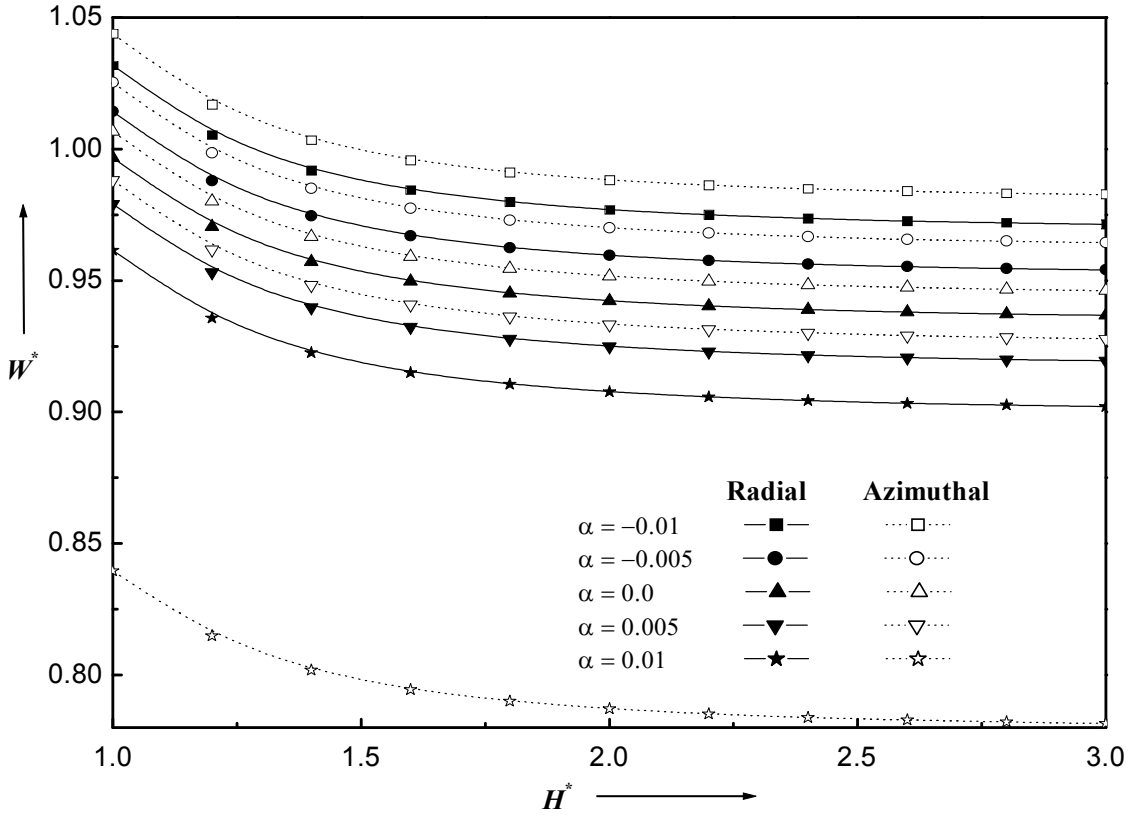

Figure 4.2 Variation of non-dimensional load carrying capacity W^* with H^* for different values of α with $K = 0.5$ and $C = 0.1$

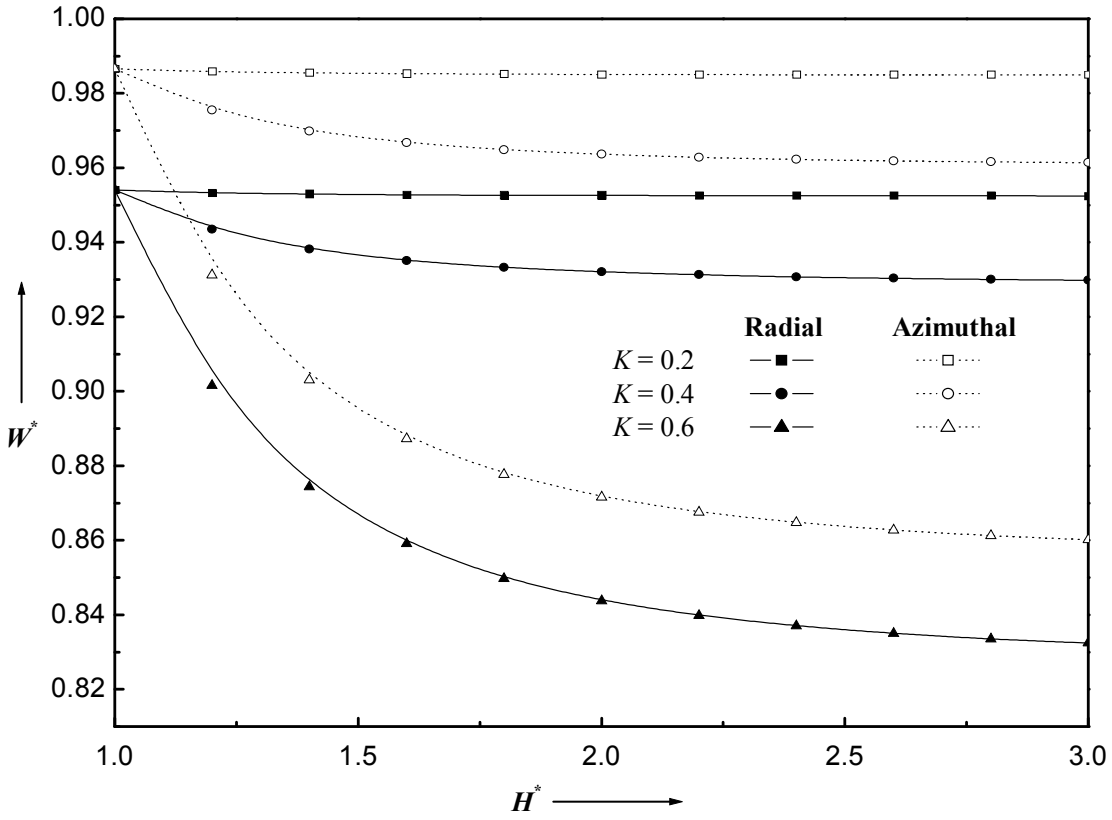

Figure 4.3 Variation of non-dimensional load carrying capacity W^* with H^* for different values of K with $\alpha = 0.01$ and $C = 0.2$

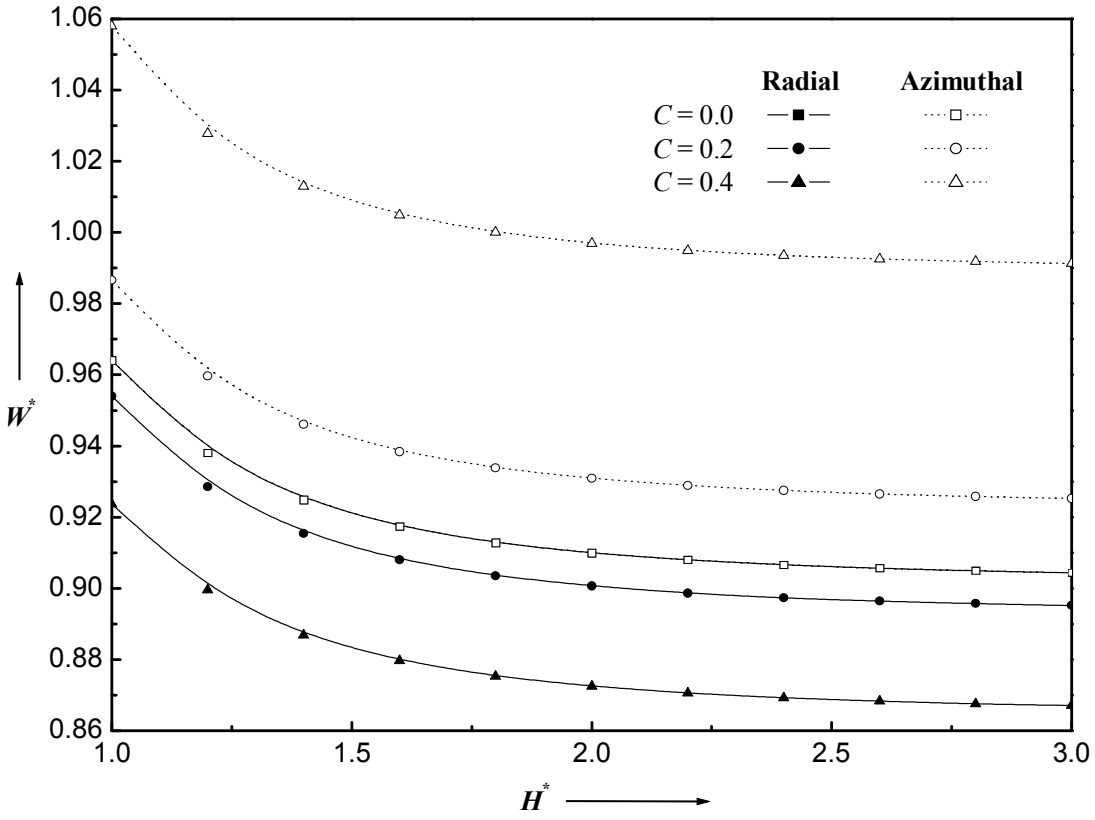

Figure 4.4 Variation of non-dimensional load carrying capacity W^* with H^* for different values of C with $\alpha = 0.01$ and $K = 0.5$

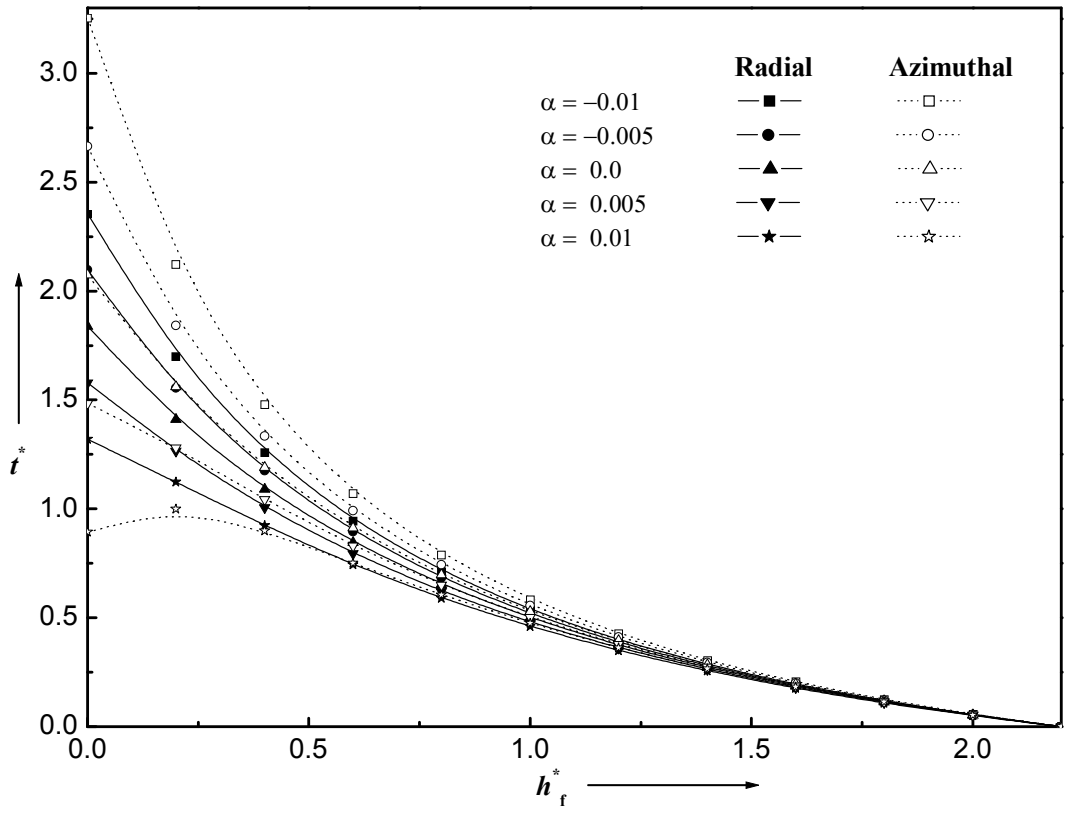

Figure 4.5 Variation of non-dimensional time of approach t^* with h_f^* for different values of α with $C = 0.2$, $K = 0.5$ and $h_3^* = 0.15$.

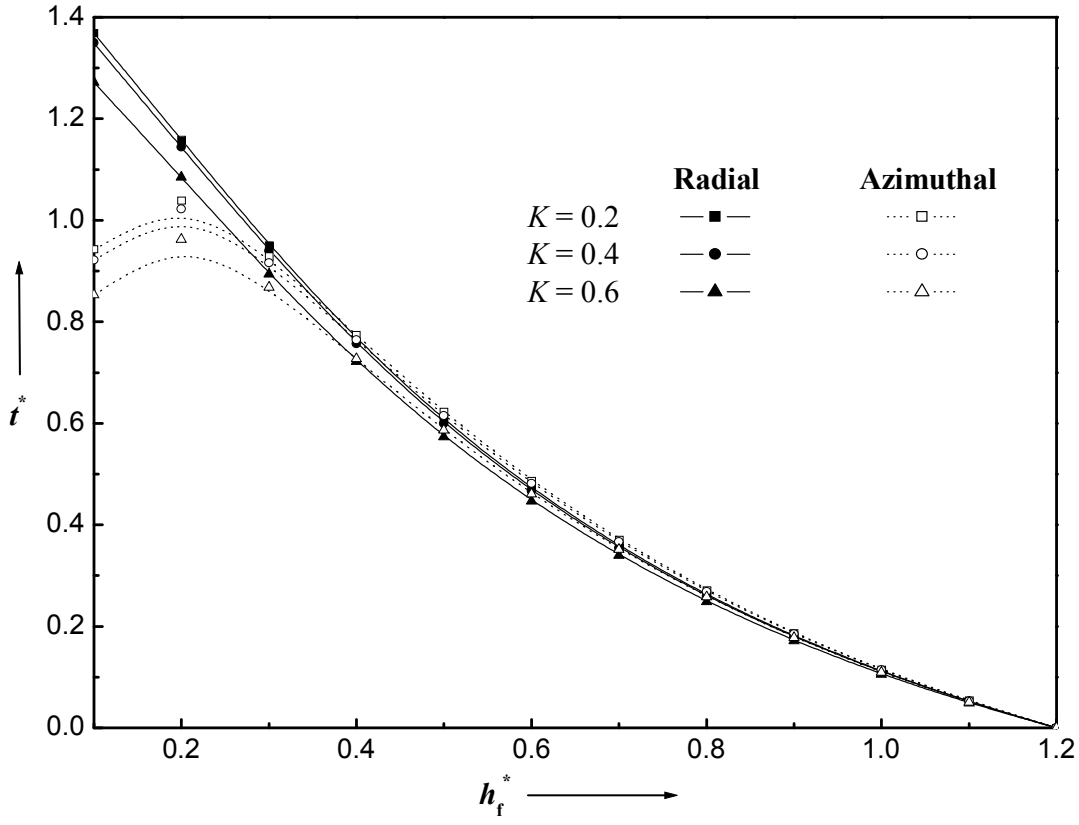

Figure 4.6 Variation of non-dimensional time of approach t^* with h_f^* for different values of K with $\alpha = 0.01$, $C = 0.2$, and $h_3^* = 0.15$

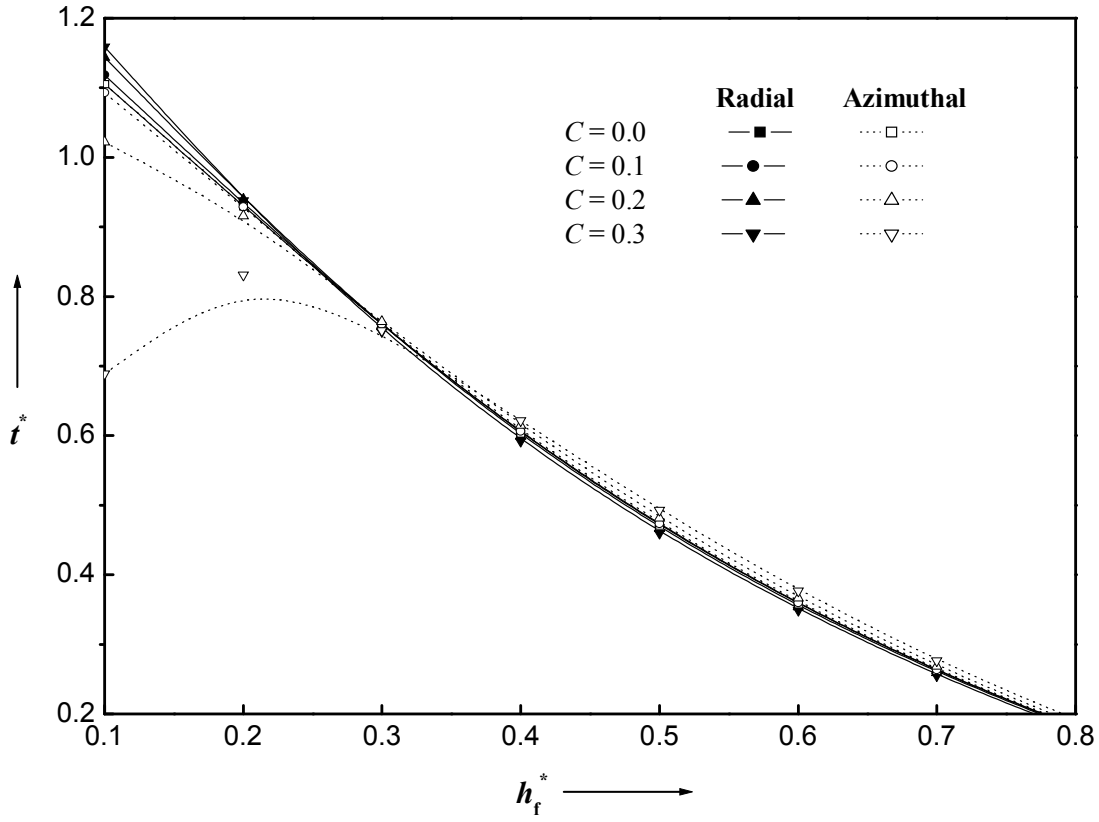

Figure 4.7 Variation of non-dimensional time of approach t^* with h_f^* for different values of C with $\alpha = 0.01$, $K = 0.4$, and $h_3^* = 0.15$.

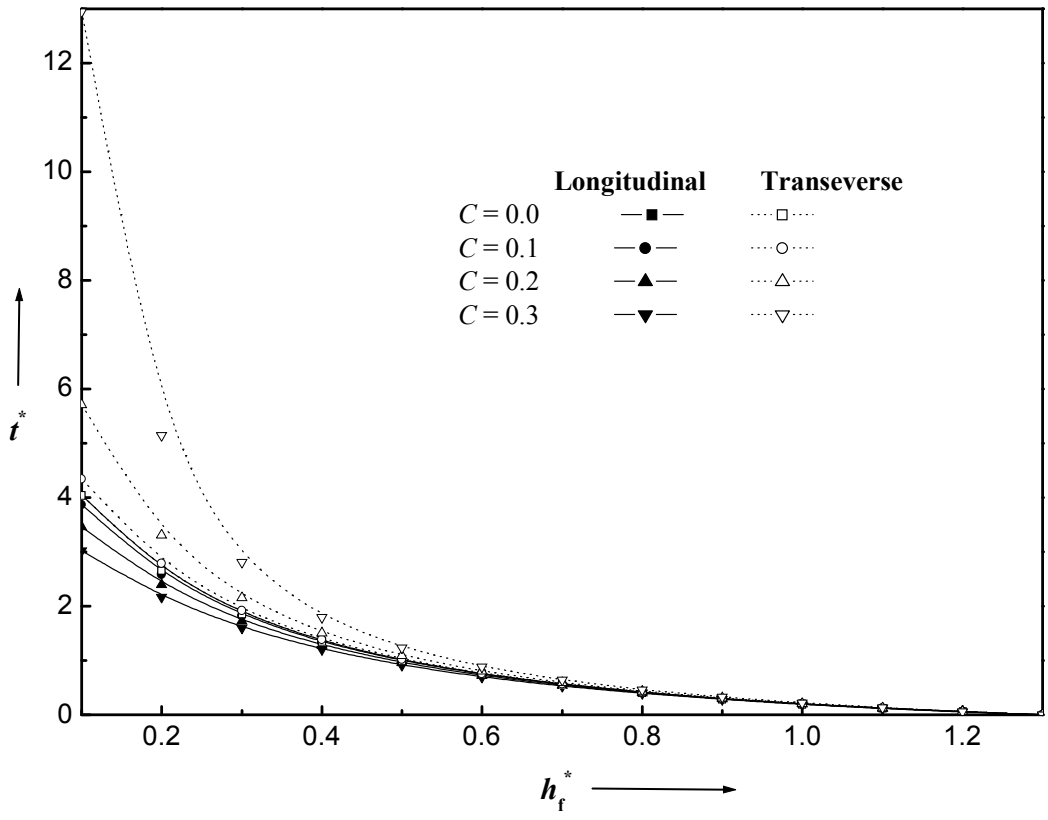

Figure 4.8 Variation of non-dimensional time of approach t^* with h_f^* for different values of C with $\alpha = -0.01$, $K = 0.4$, and